

Journal of Alloys and Compounds 425 (2006) 4-9



www.elsevier.com/locate/jallcom

# Structure and magnetic properties of Cr(N)–β-Cr<sub>2</sub>N nanoparticles prepared by arc-discharge

W.J. Feng\*, D. Li, W.F. Li, S. Ma, Y.B. Li, D.K. Xiong, W.S. Zhang, Z.D. Zhang

Shenyang National Laboratory for Materials Science, Institute of Metal Research, International Centre for Materials Physics, Chinese Academy of Sciences, 72 Wenhua Road, Shenyang 110016, People's Republic of China

> Received 6 December 2005; received in revised form 6 January 2006; accepted 10 January 2006 Available online 20 February 2006

#### Abstract

Cr(N)– $\beta$ - $Cr_2N$  nanoparticles were prepared by arc-discharge process in a mixture of argon, hydrogen and nitrogen gases. The nanoparticles are composed of the two components, i.e. Cr(N) solid–solution nanoparticles (polyhedral shape) and  $\beta$ - $Cr_2N$  nitrogen-deficiency nanoparticles (cuboidal shape). Both the nanoparticles share a similar shell-core structure: the shell consists of chromium oxide  $Cr_2(CrO_4)_3$  or Cr–O (20 at% Cr), and the complex of Cr and N–O, as well as the core of Cr(N) solid–solution or  $\beta$ - $Cr_2N$ . Moreover, the nanoparticles have a blocking temperature of 29 K and a narrow size distribution. The weak ferromagnetism can be interpreted in terms of the presence of non-compensated surface spins. For the field-cooled (FC) magnetization with the field of 0.01 T, a perfect Curie–Weiss fit of the data above 50 K indicates paramagnetic characteristics of the nanoparticles. This is supported by the hysteresis loops at 5 and 295 K. The paramagnetic Curie temperature of -124 K suggests the type of dominant interaction is antiferromagnetic.  $\bigcirc$  2006 Published by Elsevier B.V.

Keywords: Arc-discharge; Nanoparticles; Blocking temperature; Curie-Weiss law

#### 1. Introduction

Nano-scaled materials have attracted considerable interest because these materials are suitable for the investigation of some fundamentally physical behaviors under reduced dimensionality, as well as they have a number of novel promising applications [1–4]. Among these materials, magnetic nanocapsules/nanoparticles are of interest for their unique shell-core structures and remarkable properties. It is well known that the nanoparticles are easy to be oxidized, due to a large ratio of surface to volume. A number of materials, for instance, carbon [5], silica [6], aluminum oxide [7], boron oxide [8], and boron nitride [9], etc. have been employed as the encapsulating ones of the nanoparticles. For well-coated nanoparticles, the role of encapsulating materials is to prevent the core component, such as Fe, Co, and rare-earth nanoparticles, etc. from oxidation. On the other hand, chromium nitride

(CrN) with the cubic rock-salt structure has been known as a technologically important material because of its hardness, excellent resistance to corrosion, oxidation, and wear [10,11]. In fact, CrN/Cr<sub>2</sub>N has been successfully used as a protective coating appliance, e.g., wear and corrosion-resistant coating for various materials, tools, machine parts and so on [12,13]. To date, however, there have been few studies on the nanoparticles of chromium nitride (CrN/Cr<sub>2</sub>N). It may shed some lights on the study of enlarging the family of nanocapsules/nanoparticles. In our previous work [14–16], a process of arc-discharge was developed to fabricate magnetic nanocapsules/nanoparticles with different types of shell-core structures by changing either atmosphere or anode material.

In the present paper, Cr(N)– $\beta$ - $Cr_2N$  nanoparticles are prepared by arc-discharging in the mixture of Ar,  $H_2$ , and  $N_2$  gases. The microstructure and magnetic properties of the Cr(N)– $\beta$ - $Cr_2N$  nanoparticles are characterized by means of X-ray-diffraction (XRD), transmission electron microscope (TEM), X-ray photoelectron spectroscopy (XPS), and magnetic measurements, respectively.

<sup>\*</sup> Corresponding author. Tel.: +86 24 83978751 E-mail address: wjfeng@imr.ac.cn (W.J. Feng).

#### 2. Experimental procedures

The process of arc-discharge was similar to that developed elsewhere [8,14]. The anode was bulk Cr of 99.5%, while a tungsten needle of 2 mm in diameter served as the corresponding cathode. Argon (20 000 Pa) was introduced into an evacuated chamber ( $7 \times 10^{-3}$  Pa) before a potential in the range of 10–20 V was applied between the cathode and the anode. When the arc became stable with a current of 60 A, a mixture of  $N_2$  (8000 Pa) and  $H_2$  (1000 Pa), served as a reactant gas and a source of hydrogen plasma, respectively, was introduced into the chamber. During the experimental process, the current was maintained at 60 A, while the potential varied in a range of 10–20 V. Deposits on the water-cooled wall of the chamber were collected for experiments.

XRD spectra were recorded at room temperature in a D/max-yA diffractometer with Cu K $\alpha$  ( $\lambda = 1.54056 \,\text{Å}$ ) radiation and a pyrolytic monochromator. The morphology and the structure of the deposits were observed by a JEOL 2010EX TEM operating at 200 kV. Surface compositions were investigated by XPS (Witchford, UK), while Al Kα line was used as an X-ray source emitting at 1486.8 eV. The experimental conditions of each cross-section were kept the same, and only time for etching changed. The etching rate was determined by calibrations on typical materials. The etching acted approximately the same on alumina as it did on the nanoparticles in the present system. The magnetic properties of the sample were measured by a superconducting quantum interference device (SQUID, Quantum Design) magnetometer. The procedures for the zerofield-cooled (ZFC) and field-cooled (FC) magnetization measurements were as follows: For ZFC, the sample was first cooled without any magnetic field from room temperature to 5 K, then the magnetization was measured under a dc magnetic field in the warming process. For FC, the magnetization was measured while the sample was cooled in the same dc magnetic field from 350 to 5 K.

#### 3. Results and discussion

Fig. 1 shows XRD pattern of the as-prepared nanoparticles, from which, two phases, i.e. cubic Cr and hexagonal  $\beta$ -Cr<sub>2</sub>N, could be indexed. However, it should be noticed that the XRD peaks of Cr shift to lower angles while those of  $\beta$ -Cr<sub>2</sub>N to the opposite direction, which indicates a lattice expansion of the former, as well as lattice shrinkage of the latter. According to the (2 1 1) diffraction peak, the calculated lattice parameter of the as-prepared cubic Cr component is 2.887 Å, which is bigger than 2.881 Å of the raw Cr powders. This difference suggests

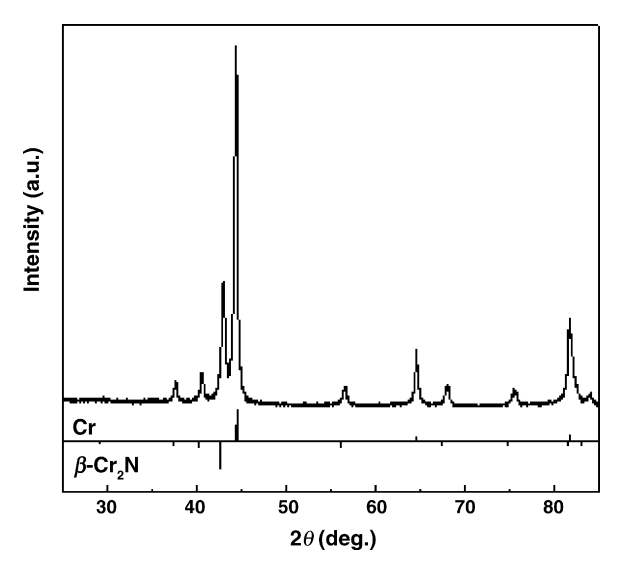


Fig. 1. XRD spectrum of Cr(N)– $\beta$ - $Cr_2N$  nanoparticles. For comparison, the corresponding XRD patterns of the Cr raw powders and the standard  $\beta$ - $Cr_2N$  phase (Card number: 35-0803) are also represented below the experimental data.

that some nitrogen atoms may enter as the solid–solution atoms into the body-centered cubic (BCC) Cr lattice. On the other hand, according to the (3 0 0) and (1 1 3) diffraction peaks of the corresponding  $\beta$ -Cr<sub>2</sub>N component, the calculated lattice parameters of  $\beta$ -Cr<sub>2</sub>N component are a = 4.776 Å and c = 4.448 Å, which are both smaller than the standard values (a = 4.811 Å and c = 4.484 Å). It seems to be indicative of nitrogen vacancies for the  $\beta$ -Cr<sub>2</sub>N component. In addition, from the half-width of XRD peaks of the two components, the particle sizes are estimated as 20–40 nm and 10–30 nm for Cr(N) solid–solution nanoparticles and  $\beta$ -Cr<sub>2</sub>N nanoparticles, respectively.

The typical morphology of the Cr(N)– $\beta$ - $Cr_2N$  nanoparticles is represented in a TEM micrograph (Fig. 2(a)). Obviously, the nanoparticles are composed of some polyhedral particles, with a size range from 10 to 50 nm, and other cuboidal ones, with a smaller size. The size of the particles is basically coincident with the results estimated from the XRD pattern. Fig. 2(b) and (c) represent the TEM images in a larger magnification of the β-Cr<sub>2</sub>N nanoparticles and the Cr(N) solid–solution nanoparticles, respectively, which are supported by two selected area electron diffractions (SAED) shown in their respective insets. The electron diffraction pattern (see the inset of Fig. 2(b)) is mainly composed of concentric diffuse rings, again suggesting the nanocrystalline nature of the particles. All the rings are indexed out, which are well coincident with some of the XRD peaks corresponding to the hexagonal β-Cr<sub>2</sub>N phase. The SAED patterns in the inset of Fig. 2(c) are also well consistent with the XRD patterns correspondent to the cubic Cr(N) solid–solution phase. Furthermore, from both the HRTEM images, one can find there is a thin coating layer around the corresponding nanoparticles. The layer can be tentatively ascribed to chromium oxide, because an oxide layer easily forms on the surface of the nanoparticles when they are exposed to air [17,18]. The reason why we have not found any traces of peaks of chromium oxides in the XRD patterns is that the oxides layer is too thin to give any detectable XRD

To obtain more information on the surface and inner chemistry, we investigate our sample with XPS. Full-scan XPS results (not shown here) have verified the presence of the Cr, N, O and C elements. Obviously, the occurrence of C element is owing to carbon dioxide of air. Fig. 3(a)–(c) represent the XPS spectra of the Cr 2p, N 1s, and O 1s electrons with the etching time of 0, 30, 90, and 210 s (corresponding to etching depths of 0, 0.9, 2.7, and 6.3 nm, respectively). For different etching depths, binding energy's (BE) intensities are changed. This expresses that the distributions of these atoms are different on each cross section [19]. The curves of Cr 2p BEs, shown in Fig. 3(a), give the distribution of the peak shapes and positions. The inset of Fig. 3(a) represents the fitting curves of the etching time 210 s for Cr 2p 574.7 eV (Cr) and 577.6 eV (Cr–O (20 at% Cr) surface non-bombarded). It should be noted that the intensity of Cr 2p 574.7 eV (Cr) becomes stronger, while that of Cr 2p 577.6 eV (Cr-O (20 at% Cr) surface non-bombarded) becomes weaker, as a function of the etching time. This suggests that the Cr atoms are inside the nanoparticles, whereas chromium oxides on the surfaces of the nanoparticles. Furthermore, according

### Download English Version:

## https://daneshyari.com/en/article/1627126

Download Persian Version:

https://daneshyari.com/article/1627126

<u>Daneshyari.com</u>